



Anal. Bioanal. Chem. Res., Vol. 4, No. 2, 307-317, December 2017.

Thermodynamic Study of the Ion-Pair Complexation Equilibria of Dye and Surfactant by Spectral Titration and Chemometric Analysis

Hakimeh Abbasi Awal, Bahar Ghasemzadeh and Abdolhossein Naseri*

Department of Analytical Chemistry, Faculty of Chemistry, University of Tabriz, Tabriz 51644-14766, Iran

(Received 19 January 2017, Accepted 12 July 2017)

Surfactant-dye interactions are very important in chemical and dyeing processes. The dyes interact strongly with surfactant and show new spectrophotometric properties, so the UV-Vis absorption spectrophotometric method has been used to study this process and extract some thermodynamic parameters. In this work, the association equilibrium between ionic dyes and ionic surfactant were studied by analyzing spectrophotometric data using chemometric methods. Methyl orange and crystal violet were selected as a model of cationic and anionic dyes, respectively. Also, sodium dodecyl sulphate and cetyltrimethylammonium bromide were selected as anionic and cationic surfactant, respectively. Hard model methods such as target transform fitting (TTF), classical multi-wavelength fitting, and soft model method such as multivariate curve resolution (MCR) were used to analyze data recorded as a function of surfactant concentration in premicellar and postmicellar regions. Hard model methods were used to resolve data using ion-pair model in premicellar region in order to extract the concentration and spectral profiles of individual components, and also related thermodynamic parameters. The equilibrium constants and other thermodynamic parameters of interaction of dyes with surfactants were determined by studying the dependence of their absorption spectra on the temperature in the range of 293-308 K at concentrations of 5×10^{-6} M and 8×10^{-6} M for dye crystal violet and methyl orange, respectively. In postmicellar region, the MCR-ALS method was applied for resolving data and getting the spectra and concentration profiles in complex mixtures of dyes and surfactants.

Keywords: Dye-surfactant interaction, Classical fitting, Target transform fitting, MCR, Absorption titration, Thermodynamic parameters

INTRODUCTION

Dye-surfactant interactions are of great interest in dyeing and photographic industries [1], biological and medicinal photosensitization [2] and in analytical [3] and environmental [4] sciences. Freshly prepared aqueous solutions of oppositely charged surfactant and dyes exhibit a broad absorption spectrum, not similar to the known spectrum of the monomeric or dimeric forms of the dye [5]. Information on interactions between dyes and ionic surfactants can add to our understanding of combined electrostatic-hydrophobic interactions [6].

The surfactants can form a complex with ionic dyes. The

addition of ionic surfactant to the solution of dye with the opposite charge often causes the formation of ion-pair complexes that may be insoluble or soluble complexes. The precipitation of insoluble complexes in dyeing baths can be prevented by adding the ionic surfactant at a concentration higher than the critical micelle concentration (CMC) to the solution [7]. Thus, it is necessary to understand the nature of interactions between surfactant and dye molecules and also the ratio of dye to surfactant concentration in these baths in order to design desirable dye-surfactant systems [7].

The UV-Vis absorption spectroscopy is one of the most suitable methods for studying the association chemical processes [8,9]. It was noticed that color of dyes changes upon addition of detergents, and this effect occurs only when the charge on the detergent aggregate is opposite in

*Corresponding author. E-mail: a_naseri@tabrizu.ac.ir

sign to that on the dissociated dye molecule. This behavior was proved to be quite general [10] and is attributed to the formation of dye-surfactant salt, ion pair, molecular complex, dye-rich induced micelles aggregation of dye-surfactant complex and change in chromophore microenvironment [11-13]. These changes in chromophore induce spectral changes. The nature of the dyes and their own tendency to aggregate [13] has to be considered to explain such phenomena. It appears that at pre-micellar surfactant concentrations complex dye-surfactant aggregates are formed and at post-micellar concentrations the aggregates are ruptured into dye incorporating into the micelles. The existence of true ion-association complexes formed below the CMC between ionic surface active agents and dye with an opposite charge is supported by most of the published data [14]. At surfactant concentrations, at CMC value and above, the solubilizing effect of the micelles begins to be important, and most likely the ion-association complexes are incorporated into the micelles. Accordingly, some new changes in spectral responses have been reported [15].

In the presence of surfactants, considerable changes in the state of the dye in solution and morphological changes influence both the thermodynamics and kinetics of dyeing. So, investigations on the behavior of natural dye in an aqueous surfactant solution can provide useful information for understanding the thermodynamics and kinetics of the dyeing process by the natural dyes [10,16-18]. The thermodynamic process of the interaction of dye with surfactants and transfer of the dye between micellar and bulk water phases is characterized by free energy changes, binding constant and partition coefficients, respectively.

With proper chemometric approaches, spectroscopic data can be resolved, and thus, the spectrum of each component and thermodynamic parameters can be obtained simultaneously. Model-based methods and model-free methods are two main branches in chemometrics. Model-based methods including classical model fitting or non-linear least-squares fitting (NLLS) [19], rank annihilation factor analysis (RAFA) [20,21], and target transform fitting (TTF) [22,23] are commonly used. An important point in usual model-based methods is that the considered system must be well defined which is not fulfilled in most cases.

Indeed, although utilizing model-based methods has some advantages such as robustness and higher reliability compared to soft-model methods, mentioned drawback prevents utilizing such approaches in most cases. A series of model-free methods are developed which do not require a detailed thermodynamic description, but takes into account the features of the multidimensional data itself and general knowledge such as mass balance. Using model-free methods we avoid the errors caused by selecting an incorrect model. Gemperline *et al.* [24] and Zhu *et al.* [25] processed the *in situ* spectroscopic data using iterative target transformation factor analysis (ITTFA) to estimate composition profiles and pure component spectra. Some modified ITTFA methods were proposed to resolve the undetectable components in the chemical reaction [26,27]. In addition, the multivariate curve resolution-alternating least squares (MCR-ALS) approach was proposed by Saurina *et al.* [28] to handle the model-free problem in monitoring chemical reaction processes [29]. This approach was employed by Tauler and his research group to deal with a variety of issues [30,31].

Several approaches have been proposed for the analysis of multivariate data. Most of them have been based on the postulation of a chemical model [32], *i.e.* analysis of experimental data by assuming a previous knowledge of the system in pre-micellar regions. In such cases, equations for both complexation equilibria and shape of the recorded absorption spectra for individual species are available in pre-micellar region. After determination of equilibrium constant, thermodynamic parameters, ΔH° , ΔS° and ΔG° can be realized using Van't Hoff equation. In this work, classical model fitting and target transform fitting are used as hard-model based data analysis methods to analyze the recorded absorption spectra in a successive ion-pair complex system. The proposed methods were used to calculate the equilibrium constant, ΔH° , ΔS° and ΔG° of surfactant-dye interactions processes of crystal violet (CV) with SDS and methyl orange (MO) with CTAB. Since the nature of the aggregation behavior of surfactant in post-micellar region is not yet well understood, and finding a robust model for these systems is a difficult task requiring some physicochemical parameters, we preferred to apply a SMCR method for resolving the spectra and concentration

profiles in complex mixtures of dyes and surfactants.

MATERIALS and METHODS

Material and Chemical Reagents

All experiments were performed with analytical grade chemicals and doubly-distilled water. The investigated dyes, methyl orange and crystal violet, and two surfactants, sodium dodecylsulphate, and cetyltrimethylammonium bromide were purchased from Merck. All the products were used without additional purification. A stock solutions of MO (1×10^{-3} M) and CV (1×10^{-3} M) was prepared by dissolving solid dyes in water and stored in dark. Stock solution of SDS (1×10^{-2} M) and CTAB (1×10^{-2} M) was prepared by dissolving an appropriate amount of the surfactants in water. In all experiments, the ionic strengths were maintained constant by KCl (Fluka) at 0.1 M solutions of the salt. Other solutions were prepared by adding different concentrations of surfactant to a certain concentration of the dye.

Apparatus, Instrumentation and Software

The absorption spectra were measured with a double beam UV-Vis spectrophotometer (SHIMADZU, Kyoto, Japan) model UV-1601 PC with quartz cell of 1 cm path length, connected to IBM compatible computer. The software was UV-PC personal spectroscopy software version 3.7. The spectral band width was 2 nm and wavelength-scanning speed 280 nm min^{-1} . The temperature of the cell was kept constant using thermo circulating bath (Lab. Companion) model BW-050G. The calculations associated to the MCR-ALS method were performed using several programs implemented in MATLAB 2013 and obtained from MCR Web site [33]. Grid search minimization and TTF algorithm were written by authors.

RESULTS AND DISCUSSION

Nature of the Dye-surfactant Interaction

Since surfactants can form aggregates with a similar behavior to micelles, it is thus expected that surfactants with a large cationic site behave in a similar manner towards anionic dyes. Also, the surfactants with a large anionic site behave in a similar manner towards cationic dyes. In other

words, it is expected that surfactants form ion pairs with these dyes. In addition to electrostatic interaction, another kind of interaction can be considered between surfactant aggregates and the dye moiety (hydrophobic interaction), in which the microenvironment of the dye may be changed from that existing in the bulk aqueous phase, and this change can also be responsible for spectral shifts. For this purpose, we selected the interaction between crystal violet, as a cationic dye, with sodium dodecyl sulfate, as an anionic surfactant, and also methyl orange, as an anionic dye, with cetyltrimethylammonium bromide, as a cationic surfactant, for studying their interaction. The processes are addressed in detail in premicellar and postmicellar concentration range.

Dye-surfactant Interaction in the Premicellar Region

Effect of surfactant. The variation in absorption spectrum for a constant amount of dye in the presence of various concentrations of surfactant ranging from premicellar to postmicellar region is recorded between 400 to 700 nm for CV with SDS and 300 to 600 nm for MO with CTAB in different temperatures. The recorded absorption spectra are shown in Fig. 1 for both systems after fixing the temperature at 293 K. The SDS concentration for this purpose was varied from 0 to 4×10^{-4} M for a fixed concentration of CV (5×10^{-6} M). In Fig. 1 a, the addition of concentrations of SDS clearly lower than CMC to CV solution results in a clear modification of absorption spectrum. These variations in the CV absorption spectrum can be observed more clearly as the SDS concentration changes, taking into account the ratios between maximum and shoulder absorbance. Absorbance at 591 nm decreases and the shoulder becomes somewhat prominent after being blue-shifted to 553 nm. The band at 553 nm is attributable to the formation of 1:1 complex between CV and SDS.

Similar results were obtained for system of MO with CTAB in Fig. 1b. The difference is in the CMC values and the separation of absorption bands in the premicellar region of the surfactants. The CTAB concentration for this purpose was varied from 0 to 4×10^{-5} M for a fixed concentration of MO (8×10^{-6} M). According to Fig. 1b, MO has an absorption maximum at 463 nm. A new absorption spectrum is seen with the addition of concentrations of

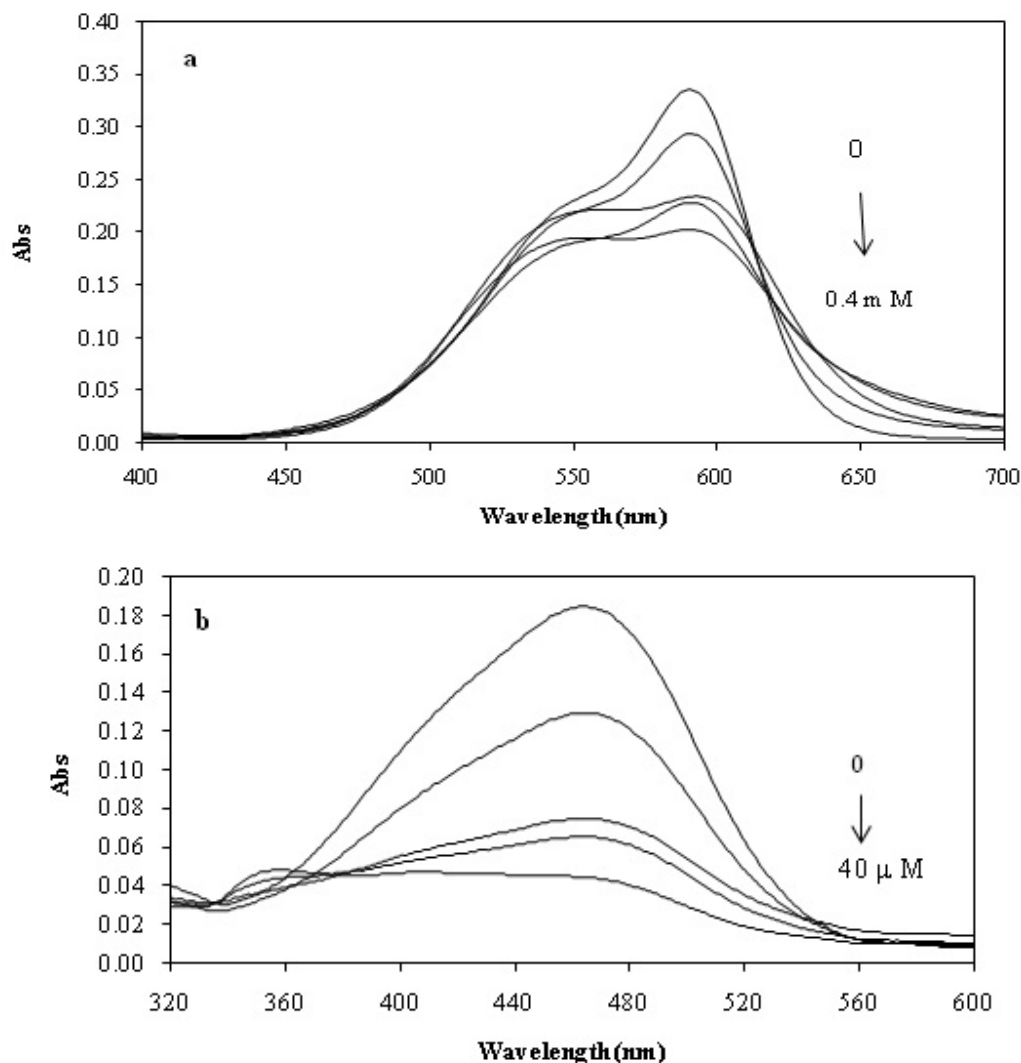


Fig. 1. (a) Absorption spectra of Crystal violet (5×10^{-6} M) at various concentrations of SDS (0 to 0.4 mM) in the premicellar region at 293K. (b) Absorption spectra of Methyl orange (8×10^{-6} M) at various concentrations of CTAB (0 to 40 μ M) in the premicellar region at 293K.

CTAB clearly lower than CMC at 369 nm with gradual decrease in the intensity of the 463 nm band. The band at 369 nm is attributable to the formation of 1:1 complex between MO and CTAB.

The results of rank analysis of individual experimental data matrices of spectra using the singular value decomposition (SVD) are given in Table 1 for both systems.

The first two singular values are much larger than the following ones. Also, the ratio between the consecutive

singular values shows that the second singular value is very larger than the third one (see S_2/S_3 ratios). So, the obtained results of SVD and also normalizing the spectra show that only two species involved in both systems are absorbent.

Analysis of Spectral Data Matrices with Model-based Methods

TTF and classical model fitting are models based on the non-linear least squares methods. Analyzing by these

Table 1. Rank Analysis of Data Matrices by SVD in Premicellar Region

| Matrix ^a | Singular values | | | | | Singular value ratios | | | |
|---------------------|-----------------|----------------|----------------|----------------|----------------|--------------------------------|--------------------------------|--------------------------------|--------------------------------|
| | S ₁ | S ₂ | S ₃ | S ₄ | S ₅ | S ₁ /S ₂ | S ₂ /S ₃ | S ₃ /S ₄ | S ₅ /S ₆ |
| D ₁ | 6.66 | 0.51 | 0.05 | 0.03 | 0.02 | 12.88 | 10.00 | 1.5 | 1.20 |
| D ₂ | 2.56 | 0.23 | 0.02 | 0.01 | 0.01 | 11.03 | 9.33 | 1.40 | 1.0 |

^aD₁ is a data matrix containing absorption spectra of crystal violet at various concentrations of SDS and D₂ is a data matrix containing absorption spectra of methyl orange at various concentrations of CTAB in the premicellar region.

methods requires bilinear data matrix as a prerequisite [34]. For studying a complexation system where surfactant is a titrant, a data matrix can be formed by arranging the absorption spectra at different concentrations of the surfactant. Such matrix will have as many rows as the number of recorded absorption spectra and as many columns as scanned wavelengths during each measurement. Estimating model's parameters using any fitting methods includes finding parameters that minimize the difference between calculated data using model function and the actual measurement. TTF performs this by projection of target vectors obtained from the model function (included parameters) into the relevant dimension of the data matrix (row space or column space). Therefore, each target vector can be tested for its presence in the data matrix by the following equations [34]:

$$r_B = t_B - t_{B,proj} = t_B (I - V^T V) \quad (1)$$

$$r_C = t_C - t_{C,proj} = (I - U U^T) t_C \quad (2)$$

where B and C subscripts indicate target vectors related to row space and column space, respectively, *r* is the residual vector, *t* is model based target vector, *t_{proj}* is projected target vector in data space, *I* is the identity matrix, and both *V* and *U* are matrices resulted from performing singular value decomposition (SVD) on data matrix and related to the row and column space of the data matrix, respectively. If the target vector (*t*) is a part of a subspace of the data matrix, then the residual vector (*r* = *t* - *t_{proj}*) will be negligible. Plotting the logarithm of length of the residual vector,

log(ssq), as a function of log(*K_b*), creates a minima for each set of equilibrium constant. This minimum is the new and hopefully better estimate for *K_b*.

As stated before, in the present case, where new absorption bands appear, the dye spectra clearly suggests the formation of a dye-surfactant complex such as [D⁺-S⁻] or [D⁻-S⁺] species. According to this fact that the binding of surfactant to dye is an equilibrium, Eq. (3) and Eq. (4) can be established:



$$K_b = \frac{[\text{Complex}]}{[\text{Dye}][\text{Surfactant}]} \quad (4)$$

where *K_b* is the binding constant interaction of dye and surfactant in solution. By assuming [Complex] = [*C_b*], [Dye] = [*D_f*], [Surfactant] = [*S_f*] and mass balance Eq. (5) and Eq. (6) we have Eq. (7):

$$[D_f] = [D_T] - [C_b] \quad (5)$$

$$[S_f] = [S_T] - [C_b] \quad (6)$$

$$K_b = \frac{[C_b]}{([D_T] - [C_b])([S_T] - [C_b])} \quad (7)$$

where *D_T* and *S_T* are the analytical concentrations of dye and surfactant in solution, respectively. So, quadratic equation in terms of free dye concentration [*D_f*] can be obtained as Eq. (8):

Table 2. Thermodynamic Parameters for the Interaction of Dyes with Surfactants in Premicellar Region

| System | T (K) | Log K_b^a | Log K_b^b | ΔH° (kJ mol ⁻¹) | ΔS (J mol ⁻¹ K ⁻¹) | ΔG° (kJ mol ⁻¹) |
|-----------------|----------|-------------|---------------------|---|--|---|
| CV with SDS | 293 | 3.95 | 3.91 (± 0.07) | -54.11 | -108.11 | -22.43 |
| | 298 | 3.86 | 3.86 (± 0.05) | | | -21.89 |
| | 303 | 3.76 | 3.76 (± 0.08) | | | -21.35 |
| | 308 | 3.39 | 3.39 (± 0.11) | | | -20.81 |
| MO with CTAB | 293 | 5.22 | 5.22 (± 0.10) | -113.83 | -289.44 | -29.02 |
| | 298 | 4.91 | 4.91 (± 0.07) | | | -27.57 |
| | 303 | 4.53 | 4.53 (± 0.12) | | | -26.12 |
| | 308 | 4.03 | 4.03 (± 0.09) | | | -24.68 |

^aThe results obtained by TTF. ^bThe results obtained by multi-wavelength classical fitting.

$$K_b [D_f]^2 + [D_f](K_b [D_T] + K_b [S_T] + 1) - [D_T] = 0 \quad (8)$$

TTF was combined grid search method in order to find the binding equilibrium constants. A particular MATLAB optimization function using "root" command in Eq. (8) was used to optimize all of concentration profiles. Since K_b value of each ion-pair complex system is completely independent, it can be obtained by TTF or by classical model fitting.

So, $\log K_b$ was searched in the range of 1-10 for both systems at four temperatures 293, 298, 303 and 308 K, separately. The results are shown in Table 2 for both selected systems. As expected, K_b decreases with increasing temperature, while it is virtually independent of total dye concentration. The increase in the temperature of solution causes a reduction in the binding constant that it is due to the weakening of interactions between dye and surfactant molecules at high temperatures. Using initial concentrations of $[D_T]$ and $[S_T]$, the equilibrium species concentrations $[D_f]$, $[S_f]$ and $[C_b]$ were obtained for each equilibrium. Then, related spectral profiles retrieved in each of the temperatures by least square.

The theory of classical multi-wavelength model fitting is available in the literature and is explained here briefly [19,30,34]. Assume a two-way spectrophotometric

complexometric data (monitored reaction at $n\lambda$ wavelengths), D , is decomposed into the product of C , containing concentration profiles and S of absorption spectra:

$$D = CS^T + R \quad (9)$$

The matrix R is a collection of the residuals, the difference between the measurement D and its calculated representation CS^T . In hard model analysis, the aim is finding the set of parameters according to Eq. (10) so that the sum over all the squares, ssq , over all the elements of the error matrix, R , is minimal.

$$ssq = \sum R_{i,j} = f(k_b) \quad (10)$$

The 2nd order equation of (8) was solved, and, therefore, the matrix C (concentration profile) by initial estimation of equilibrium constants was established. Using least squares ($S^T = C^+D$, where C^+ is the pseudo-inverse of the matrix C) the spectra of included components were estimated. Then, the sum of squares can be defined as a function of only the nonlinear parameters (e.g., the equilibrium constants) as Eq. (10) which has been derived using Eq. (11):

$$\text{ssq} = f(K_b) = D - CS^T = D - CC^+D, \quad (11)$$

where K_b is the vector of nonlinear parameters, as defined by the chosen model. Any method that performs this minimization task, can be applied. In this work, the Newton-Gauss-Levenberg-Marquardt algorithm (NGLM) was applied because it is fast, robust and additionally delivers basic statistical analysis of the resulting parameters. The results are shown in Table 2 for both selected systems.

Thermodynamic Analysis for Binding between Dye and Surfactant

Small molecules are bound to macromolecule mainly by four acting forces: hydrogen bond, van der Waals force, electrostatic force, and hydrophobic interaction force. The thermodynamic parameters, enthalpy change (ΔH°), entropy change (ΔS°), and free energy change (ΔG°) of the reaction are important parameters for confirming binding mode. Thus, in order to further characterize the acting forces between dye and surfactant, the thermodynamic parameters were obtained.

If the enthalpy change (ΔH°) does not vary significantly over the temperature range studied, the thermodynamic parameter of ΔH° , entropy change (ΔS°) and free energy (ΔG°) can be determined from the Van't Hoff equation:

$$\ln K_b = -\frac{\Delta H^\circ}{RT} + \frac{\Delta S^\circ}{R} \quad (12)$$

where K_b is the binding constant and R is the gas constant. The values of ΔH° and ΔS° were calculated from the slope and intercept of the plot of $\ln K_b$ vs. $1/T$, respectively.

The value of free energy change was evaluated using the Gibbs-Helmholtz equation given by Eq. (13):

$$\Delta G^\circ = \Delta H^\circ - T\Delta S^\circ \quad (13)$$

The equilibrium constants at different temperatures and thermodynamic parameters of the reactions of the dyes are listed in Table 2. All the ΔG° values are negative, indicating that the junction is spontaneous. Moreover, the ΔG° values increase with increasing the temperature for binding process. This means that binding of dye to surfactant is highly spontaneous at lower temperatures. All the ΔH°

values are negative indicating that binding process is exothermic. Binding of dye to the surfactant is accompanied by the negative ΔS° values. This means that entropy is decreased due to the binding of dye molecules to the surfactant and forming of ion pair complexes. The values of thermodynamic parameters also indicates that interaction of the MO dye with the cationic surfactant CTAB is more favorable in comparison with CV dye with anionic surfactant SDS.

Dye-surfactant Interaction in Postmicellar Region Analysis of Spectral Data Matrices with MCR-ALS

As explained previously, the absorbance changes in above of the CMC is different from the blow of CMC. The Sample absorption spectra are shown in Fig. 2 for both systems in temperature 293 K. The spectra were recorded for three different temperatures 298, 303 and 308 K. The results of rank analysis of individual experimental data matrices of spectra using the singular value decomposition (SVD) are given in Table 3 for both systems. Performing SVD on the data showed the existence of three components in the solution, one of them is related to dye and another related to complex dye-surfactants and the third compound is unknown. For analyzing the data obtained in postmicellar region, the multivariate curve resolution (MCR) was used. MCR-ALS is a soft modeling method which has been shown to be a powerful tool for the spectroscopic investigations of the molecular complex formation processes [35]. The multivariate curve resolution method facilitates a bilinear decomposition of the experimental data matrix with the use of the following algebraic model of Eq. (9).

The goal of MCR-ALS is the decomposition of the data matrix, D , into the 'true' pure response profiles associated with the data variance in the rows and columns, and represented by matrices C (concentration) and S (spectra), respectively. Superscript T denotes transposition of matrix. The procedure of MCR-ALS calculates C and S in turn by the least squares, and the iterative process is repeated if the model has not been converged.

Once the number of species was extracted, the initial concentration profile and pure spectra of all the contributing species could be established by the MCR-ALS method. Initial estimates of concentration or spectral profiles are

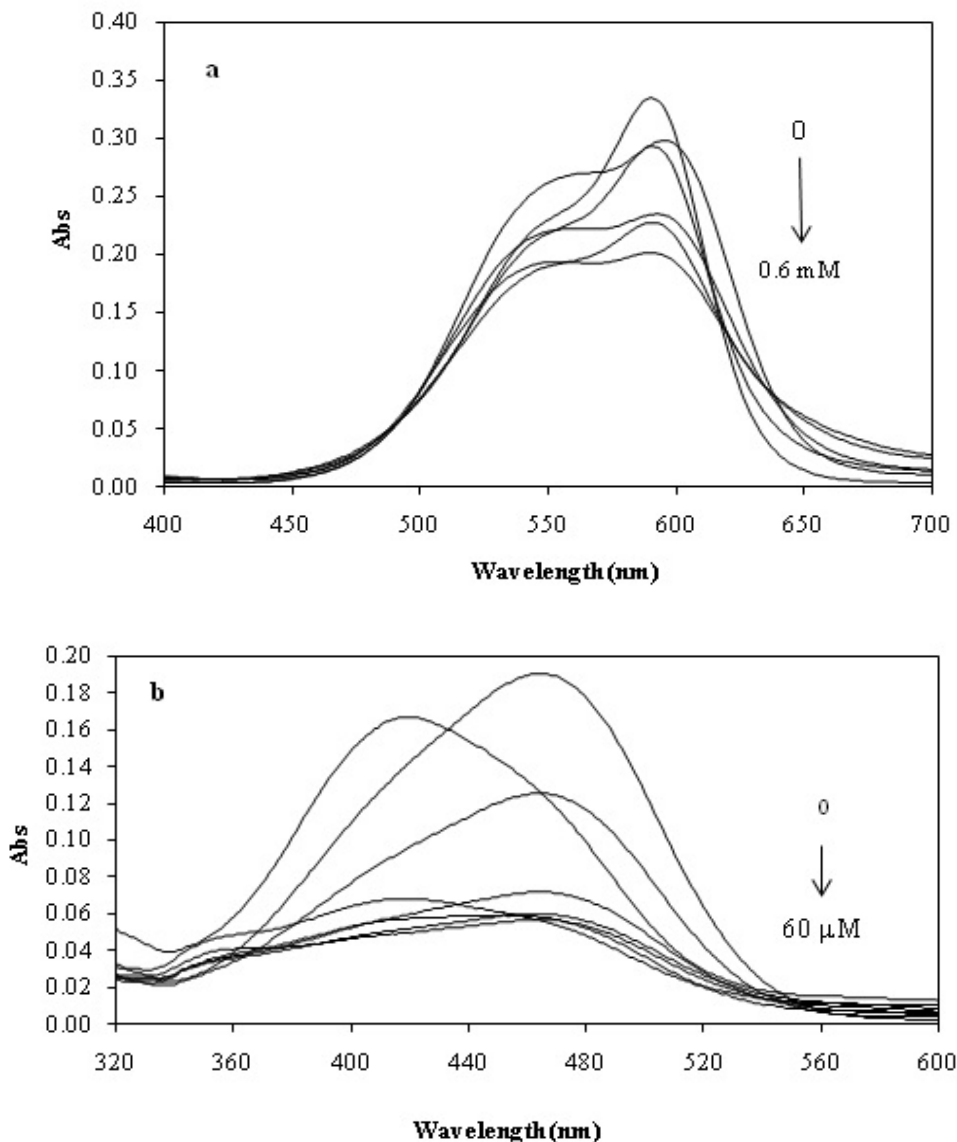


Fig. 2. (a) Absorption spectra of Crystal violet (5×10^{-6} M) at various concentrations of SDS (0 to 0.6 mM) in the micellar region at 293K. (b) Absorption spectra of Methyl orang (8×10^{-6} M) at various concentrations of CTAB (0 to 60 μ M) in the micellar region at 293K.

required to initiate the iterative ALS procedure [36], these estimations can be made using appropriate methods.

In this work, the experimental augmented data matrix was built by placing the individual data corresponding to a constant amount of dye in the presence of various

concentrations of surfactant including both premicellar and postmicellar regions recorded in the wavelength range of 300-700 nm after fixing the temperature at 293 K. This process was repeated for three different temperatures, 298, 303 and 308 K. The related bilinear model for MCR-ALS

Table 3. Rank Analysis of Data Matrices by SVD in Micellar Region

| Matrix ^a | Singular values | | | | | | Singular value ratios | | | | |
|---------------------|-----------------|----------------|----------------|----------------|----------------|----------------|--------------------------------|--------------------------------|--------------------------------|--------------------------------|--------------------------------|
| | S ₁ | S ₂ | S ₃ | S ₄ | S ₅ | S ₆ | S ₁ /S ₂ | S ₂ /S ₃ | S ₃ /S ₄ | S ₄ /S ₅ | S ₅ /S ₆ |
| D ₁ | 26.28 | 2.26 | 0.24 | 0.03 | 0.02 | 0.02 | 11.60 | 9.44 | 8.00 | 1.50 | 1.20 |
| D ₂ | 14.83 | 1.46 | 0.17 | 0.02 | 0.02 | 0.02 | 10.1 | 8.50 | 7.20 | 1.20 | 1.0 |

^aD₁ is a data matrix containing absorption spectra of crystal violet at various concentrations of SDS and D₂ is a data matrix containing absorption spectra of methyl orange at various concentrations of CTAB in the micellar region.

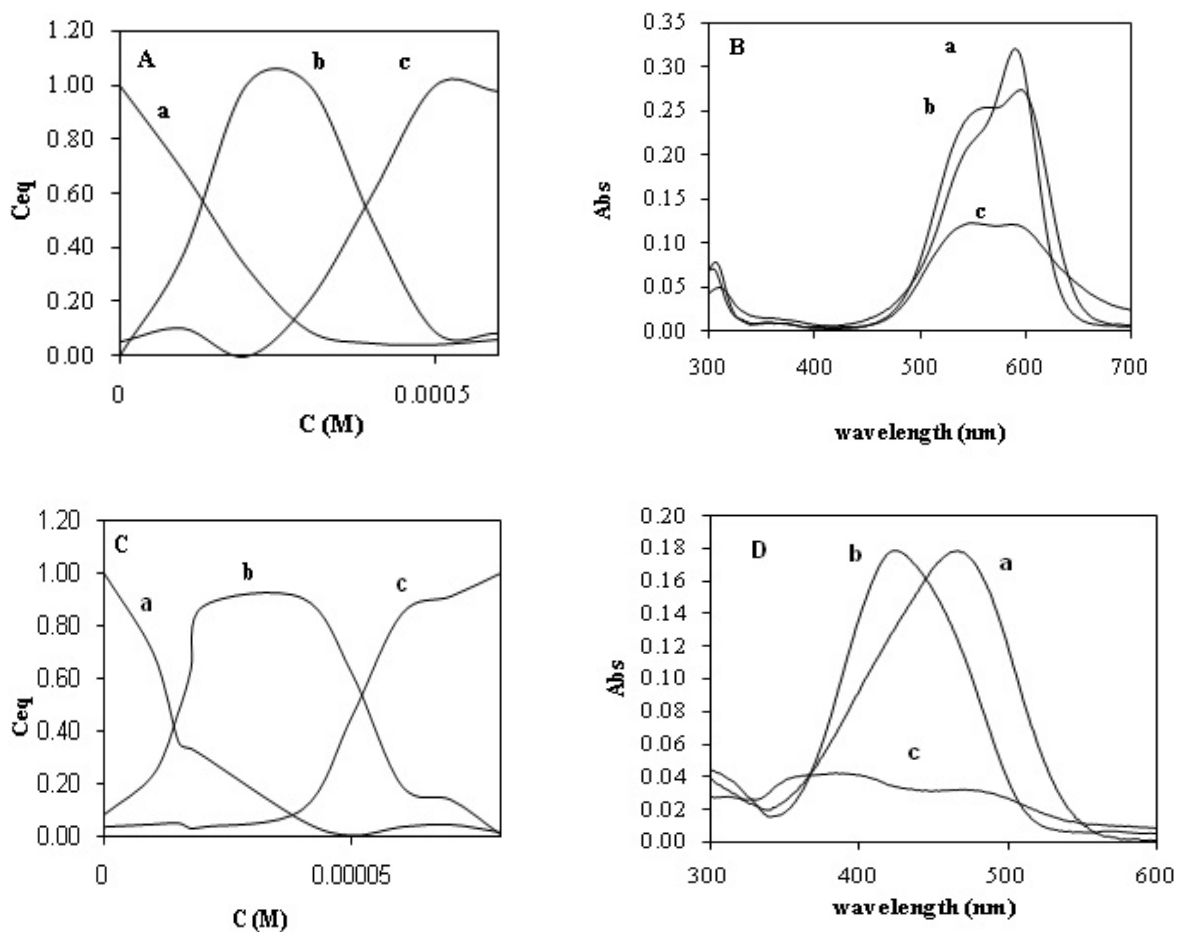


Fig. 3. Plots of the spectral and concentration profiles after MCR-ALS processing of experimental systems at 293 K. Plots (A) and (B) correspond to the spectral and concentration profiles of the interaction of crystal violet with SDS. Plots (C) and (D) correspond to the spectral and concentration profiles of the interaction of methyl orange with CTAB.

analysis is given by Eq. (14):

$$\mathbf{D} = \begin{bmatrix} \mathbf{D}^{\text{premicellar}} \\ \mathbf{D}^{\text{postmicellar}} \end{bmatrix} = \begin{bmatrix} \mathbf{C}^{\text{premicellar}} \\ \mathbf{C}^{\text{postmicellar}} \end{bmatrix} [\mathbf{S}]^T + \begin{bmatrix} \mathbf{R}^{\text{premicellar}} \\ \mathbf{R}^{\text{postmicellar}} \end{bmatrix} \quad (14)$$

Consequently, a single pure spectra matrix, \mathbf{S} , and a column wise augmented matrix of concentration profile, \mathbf{C} , can be obtained by analyzing \mathbf{D} using the MCR-ALS algorithm. The number of species, 3, was determined by SVD for \mathbf{D} . MCR-ALS analysis was started using \mathbf{S} as an initial estimate of spectra. The output spectra of TTF, pure dye and ion-pair complex, in pre micellar regions and the recorded spectrum in high concentration of surfactant in post micellar regions were used as the initial estimate.

For optimization, different constraints were applied to drive the final solution towards a chemical meaning. Non-negativity, unimodality, concentration closure and selectivity are the constraints that are used. Non-negativity constraint (for concentration and spectra profiles) forces, concentrations, and the spectra of the components so that must be positive, other constraints including closure in the dye concentration direction and selectivity constraints for reactant (pure dye) and product spectra (ion-pair complex) are also used to get unique result profiles. After applying MCR-ALS on the experimental data, concentration and the pure spectral profiles of each component in all systems can be calculated by considering a criterion for achieving a convergence point in which the difference between two successive calculated concentrations or spectral profiles becomes negligible. In Fig. 3, the concentration profiles of CV and MO at different concentrations of SDS and CTAB are illustrated. The spectral profiles obtained by MCR-ALS are reported to confirm the presence of three components in the system which signifies the presence of free dye at zero concentration of surfactant. The evolution of an intermediate component both in concentration and spectral profiles can be related to the complex formation of dye-surfactant below the CMC. However, by increasing the surfactant concentrations up to and above the CMC value, these intermediate components were consumed and new components appeared which are related to the spectra of the interacted forms of the dye with the aggregated surfactants.

CONCLUSIONS

Hard and soft models were successfully used to analyze spectrophotometric data as a function of surfactant concentration in premicellar and postmicellar regions, respectively. In premicellar regions, the results show that the evolution of a second component both in concentration and spectral profiles can be attributable to the formation of 1:1 complex between dye and surfactant. The negative ΔG° and ΔH° values point out that the binding of dye to surfactant in both systems occur spontaneously and both processes are exothermic. The results showed that the evolution of an intermediate component can be related to the complex formation of dye-surfactant below the CMC. However, by increasing the surfactant concentrations up to and above the CMC value, this intermediate component was consumed and new components appeared which are related to the spectra of the interacted forms of the dye with the aggregated surfactants.

REFERENCES

- [1] B. Simončič, M. Kert, *Dyes and Pigments* 54 (2002) 221.
- [2] B.W. Henderson, T.J. Dougherty, *Photodynamic Therapy: Basic Principles and Clinical Applications*, M. Dekker, 1992.
- [3] I. Casero, D. Sicilia, S. Rubio, D. Pérez-Bendito, *Talanta* 45 (1997) 167.
- [4] F. Merino, S. Rubio, D. Pérez-Bendito, *Analyst* 126 (2001) 2230.
- [5] P. Bilski, R. Dabestani, C. Chignell, *J. Phys. Chem.* 95 (1991) 5784.
- [6] R. Breslow, *Accounts of Chem. Res.* 24 (1991) 159.
- [7] M. Kert, B. Simončič, *Dyes and Pigments* 79 (2008) 59.
- [8] A.G. Gilani, R. Sariri, K. Bahrpaima, *Spectrochimica Acta Part A: Mol. Biomol. Spectroscopy* 57 (2001) 155.
- [9] K. Patil, R. Pawar, P. Talap, *Phys. Chem. Chem. Phys.* 2 (2000) 4313.
- [10] L. García-Río, P. Hervella, J. Mejuto, M. Parajó, *Chem. Phys.* 335 (2007) 164.
- [11] R.T. Buwalda, J.B. Engberts, *Langmuir* 17 (2001)

- 1054.
- [12] C.S. Oliveira, E.L. Bastos, E.L. Duarte, R. Itri, M.S. Baptista, *Langmuir* 22 (2006) 8718.
- [13] H.C. Junqueira, D. Severino, L.G. Dias, M.S. Gugliotti, M.S. Baptista, *Phys. Chem. Chem. Phys.* 4 (2002) 2320.
- [14] E. Iglesias, *J. Phys. Chem.* 100 (1996) 12592.
- [15] M.D. Garcia, A. Sanz-Medel, *Talanta* 33 (1986) 255.
- [16] O. Yazdani, M. Irandoust, J.B. Ghasemi, S. Hooshmand, *Dyes and Pigments* 92 (2012) 1031.
- [17] S. Chandravanshi, S.K. Upadhyay, *Color. Technol.* 128 (2012) 300.
- [18] J.B. Ghasemi, M. Miladi, *J. Chin. Chem. Soc.* 56 (2009) 459.
- [19] G. Puxty, M. Maeder, K. Hungerbühler, *Chemometr. Intell. Lab. Systems* 81 (2006) 149.
- [20] Z.-L. Zhu, J. Xia, J. Zhang, T.-H. Li, *Anal. Chim. Acta* 454 (2002) 21.
- [21] H. Abdollahi, A. Safavi, S. Zeinali, *Chemometr. Intell. Lab. Systems* 94 (2008) 112.
- [22] N.C. Imlinger, M. Krell, M.R. Buchmeiser, *Chemometr. Intell. Lab. Systems* 96 (2009) 123.
- [23] E. Furusjö, O. Svensson, L.-G. Danielsson, *Chemometr. Intell. Lab. Systems* 66 (2003) 1.
- [24] P.J. Gemperline, M. Zhu, E. Cash, D.S. Walker, *ISA Transactions* 38 (1999) 211.
- [25] Z.-L. Zhu, W.-Z. Cheng, Y. Zhao, *Chemometr. Intell. Lab. Systems* 64 (2002) 157.
- [26] Q. Zhang, X. Feng, D. Zhang, Y. Zhao, Z. Zhu, *Chemometr. Intell. Lab. Systems* 109 (2011) 131.
- [27] S.E. Richards, A.D. Walmsley, *J. Chem.* 22 (2008) 63.
- [28] J. Saurina, S. Hernández-Cassou, R. Tauler, *Anal. Chem.* 69 (1997) 2329.
- [29] M. Garrido, F. Rius, M. Larrechi, *Anal. Bioanal. Chem.* 390 (2008) 2059.
- [30] A. de Juan, R. Tauler, R. Dyson, C. Marcolli, M. Rault, M. Maeder, *TrAC Trends in Anal. Chem.* 23 (2004) 70.
- [31] S. Navea, A. de Juan, R. Tauler, *Anal. Chem.* 75 (2003) 5592.
- [32] A.K. Dioumaev, *Biophys. Chem.* 67 (1997) 1.
- [33] R. Tauler, A. De Juan, *Multivariate Curve Resolution Home Page*, 2004.
- [34] P. Jandanklang, M. Maeder, A.C. Whitson, *J. Chem.* 15 (2001) 511.
- [35] R. Tauler, A. Izquierdo-Ridora, E. Casassas, *Chemometr. Intell. Lab. Systems* 18 (1993) 293.
- [36] M. Vives, R. Gargallo, R. Tauler, *Anal. Chim. Acta* 424 (2000) 105.